

# Structural and Operational Design of an Innovative Airship Drone for Natural Gas Transport over Long Distances

G. Capitta, L. Damiani, S. Laudani, E. Lertora, C. Mandolino, E. Morra, R. Revetria

**Abstract**— The present paper illustrates the main aspects related to the conceptual design of an innovative transportation mean for natural gas. The analysis regarded the structural (stress and deformation) and technical (propulsive and structural) features as well as the overall calculation of a reduced scale (7.5 m length) airship drone prototype, able to carry out natural gas transport, contained in sealed bags, between two pre-defined departure and arrival stations, in accordance with the ENAC regulations. The proposed drone vehicle envisages the implementation of innovative solutions both for structural, motion (such as the remote control, the thermal and electric propulsion) and for materials employed.

**Index Terms** — Natural gas transport; drone airship; Logistics, Conceptual Design.

## I. INTRODUCTION

TRADITIONAL technologies, employed for gas transport from the extraction well to storage sites and utilities, are based on the use of ships and pipelines. The traditional transportation means require either a gas compression or a gas liquefying, which are very energy expensive.

To obviate this need, which involves a considerable financial outflow, the authors proposed to employ a drone airship [1], whose transportation costs, calculated in a previous work [2, 3], were found to be considerably lower than those of traditional ships, in Fig 1 the comparison is made according the averaged data over the best available configuration [2] identified according literature [3].

The mean identified in order to accomplish the transportation mission is a Lighter Than Air (LTA) drone airship of modern design. Such vehicle presents different features with respect to the traditional ones, and is named “hybrid”, as it presents aeronautical wings and a double-prolate ellipsoid form. The principle of operation is based on the Archimede’s thrust provided by the lifting gas that can be helium or hydrogen.

Although hydrogen produces an upward thrusts 10% higher compared to helium and costs less, the choice fell on the latter because it is an inert gas. Gases are stored into the airship hull, contained within impermeable gas bags. To carry out the

procedure of loading and unloading, reference was made to the well known pressure reduction plants equipped with lamination valves. Attention was paid to structural issues at rest and in flight, designing a structure able to sustain the different stresses that occur in operation, selecting the proper materials for a lighter than air vehicle.

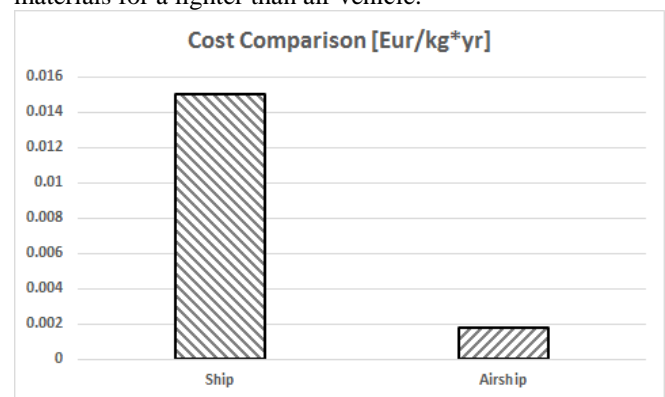


Fig. 1. Cost comparison LTA-CNG on best scenarios.

Finally, the paper shows the ENAC (Ente Nazionale Aviazione Civile – National Civil Aviation Bureau) regulations, linked to this operations typology and it analyses the main emergency scenarios with possible relative solutions to solve it.

## II. PROTOTYPE DRONE CONCEPTUAL DESIGN

The target of the present study has been the determination of the minimum size to be attributed to the blimp in order to produce a pilot prototype. As already mentioned in the previous papers, the vehicle contains gas bags for natural gas and helium (lift gas) storage. The natural gas to helium ratio was established as 60% - 40%. It is required to provide an oversized number of helium gas bags to prevent from any unforeseen event. To obtain a valid sizing, reference was made to the expression that describes the Archimedes’ principle (Eq. 1).

$$S = V_{He} (\rho_{air} - \rho_{He}) \quad (1)$$

Where:

E. Lertora is an engineer and a professor with University of Genoa, Liguria, Italy (e-mail: Enrico.Lertora@unige.it)

C. Mandolino is a researcher at Genoa University, Italy (e-mail: Chiara.Mandolino@unige.it).

R. Revetria is an engineer and a professor with University of Genoa, Liguria, Italy (phone: 3339874234; e-mail: r\_revetria@hotmail.com)

E. Morra is a freelancer engineer of Turin, Piemonte, Italy (phone: 3391505847; e-mail: e.morra@hotmail.it).

Manuscript received July 27, 2017; revised August 02, 2017.

This work was supported in part by the University of Genoa.

G. Capitta is a student of the University of Genoa, Liguria, Italy (phone: 3479633414; e-mail: gianlu93@fastwebnet.it).

L. Damiani is a researcher at Genoa University (phone +393489194710, e-mail Lorenzo.Damiani@unige.it).

S. Laudani is a student of the University of Genoa, Liguria, Italy (phone: 3334345640; e-mail: laudani.stefano@gmail.com).

- $S$  is the flotation thrust, expressed in kg;
- $V_{He}$  is the transported helium volume, expressed in  $m^3$ ;
- $\rho_{air}$  is the air density at cruising altitude, expressed in  $kg/m^3$ ;
- $\rho_{He}$  is the helium density, expressed in  $kg/m^3$ .

The helium volume is closely related to the size of the airship, therefore, an iterative procedure was adopted with the aim of obtaining a flotation thrust greater than the total weight of the mean. In this way the size of a single ellipsoid was identified: major axis of 7.5 m and minor axis of 2.5 m (Fig. 2.).

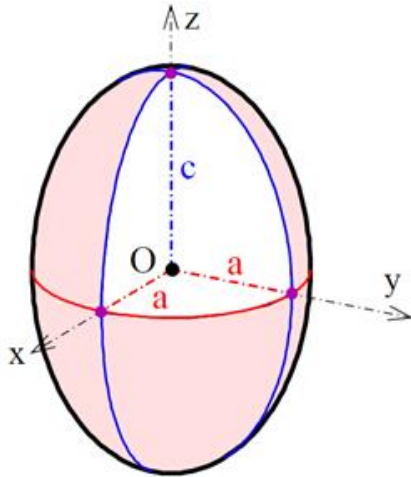


Fig. 2. Prolate ellipsoid: the two lower drive shafts have equal length.

### III. STRUCTURAL ANALYSIS AND MATERIAL SELECTION

In this section are presented the structural sizing aspects and the materials chosen for the airship drone realization. In particular, the aspects regarding the hull supporting structure and the nacelle were highlighted. Structural sizing was carried out following the procedures elaborated for submarine hulls.

For the realization of the airship, different types of materials were chosen. The internal structure is made of composite material, the Artboard / Recore, a phenolic resin foam reinforced with glass fibers. It presents important properties including light weight, high stiffness, ease of bonding and traction, wear, vibration and fire strength. For the sizing of the frame the theory of A. R. Bryant has been considered concerning the internal structure of submarines, for the similarity with the airships. Considering a single ellipsoid, the frame is composed of fourteen coaxial and equidistant rings having an "I" transversal section; the annular profiles are connected via strips and follow the ellipsoid line. Moreover, with the same method, the two ellipsoid structures are joined through a link involving the four central rings (Fig. 3.)

The authors chose to approximate the internal structure of the two ellipsoids with a cylindrical support equipped with equidistant annular ribs and equipped with bottoms at the extremities. The analytical calculations considers the behavior of a cylindrical trunk comprised between two ribs. Fig 3 provides an internal view of the ellipsoid internal structure.

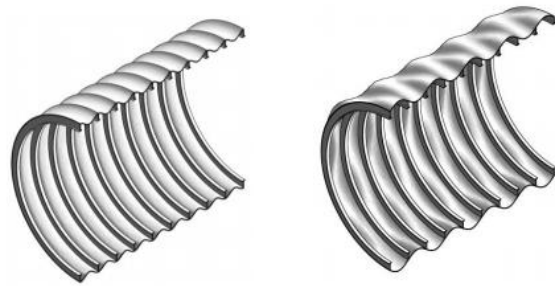


Fig. 3. Ellipsoid internal structure and predicted deformation under axial stress.

Owing to the stresses in flight, the structure is subjected to general instability, consisting in an anelastic collapsing involving both the ribs and the transversal reinforced structures. This kind of collapse is strongly influenced by the structure moment of inertia, by the imperfections in the ribs circularity and by the cylindrical structure length to diameter ratio.

The air resistance pressure experimented during flight tends to compress axially the ellipsoidal structure, and can be calculated by the aerodynamic formula:

$$p_{es} = \frac{1}{2} \rho_{air} C_x (v_v + v_w)^2 \quad (1)$$

where

- $p_{es}$  is the axial pressure exerted on the ellipsoid;
- $\rho_{air}$  is the air density at the cruise altitude;
- $C_x$  is the aerodynamic resistance coefficient;
- $v_v$  and  $v_w$  are respectively the blimp and the wind speed.

In the examined case the authors considered a cruise speed of 40 km/h and a maximum possible wind speed of 70 km/h (respectively, 11 and 19 m/s). The resistance coefficient was set 0.022.

In order to evaluate the structural characteristics of the airship a complete stress analysis was conducted on the basis of the current available literature [12] and models [13-15].

To determine the number of structural ribs to be employed and their cross-section reference was made to the Kendrick simplified formula (see Equation 2) for finding the general instability critical pressure value allowable,  $p_{cr}$ . In the equation are clearly highlighted the contributions provided by the ribs (first term of the sum in Eq. 2) and that owing to reinforcements (second term).

$$p_{cr} = \frac{E_p h}{r} \frac{\lambda^4}{\left(n^2 - 1 + \frac{\lambda^2}{2}\right) (n^2 + \lambda^2)^2} + \frac{(n^2 - 1) E_a J_{x0}}{R^3 L_f} \quad (1)$$

where (see also Fig.4):

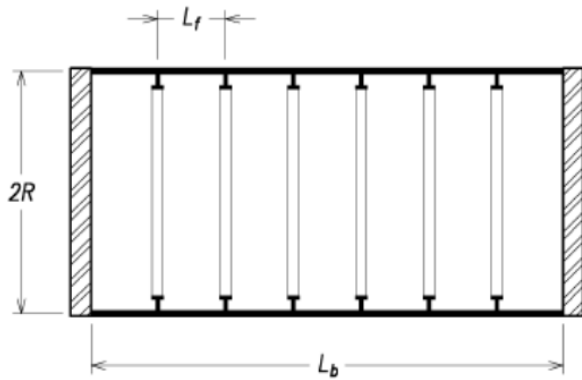


Fig. 4. Notation adopted for geometry.

- $p_{cr}$  is the critical pressure for general instability;
- $E_p$  is the Young module of the material (polyurethane);
- $E_a$  is the Young module of the plastic material (Artboard Recore)
- $J_{x0}$  is the moment of inertia of the reinforcement section around the axis passing through the section center of mass. A T profile was selected, in order to increase the contact surface between ribs and polyurethane;
- $h$  is the casing thickness;
- $R$  is the radius of the cylinder circumscribed to the ellipsoid;
- $\lambda$  is a non-dimensional parameter depending on  $R$  and  $L_b$  ( $\lambda = \pi R / L_b$ );
- $L_f$  is the ribcage interval.
- $n$  is the number of lobes, assumed equal to 2, considering an oval deformation of the centerline

The number of ribs and their cross section (see Fig.5) were determined considering a safety factor  $p_{cr}/p_{es} = 1.5$ .

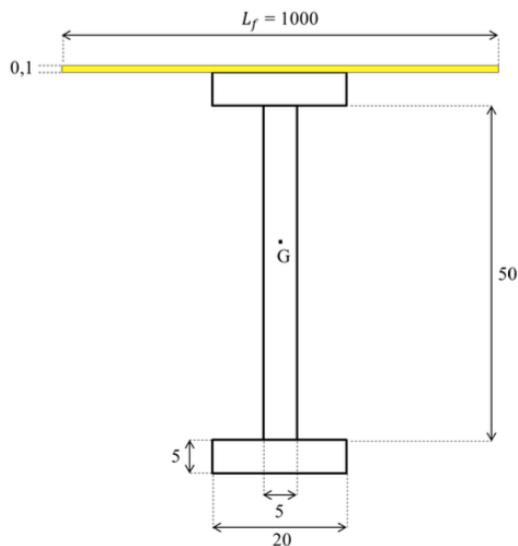


Fig. 5: Rib section (size in mm).

The sizing of the reinforcement annular ribs requires a verification to the compression status resulting from the axial compression (due to the aerodynamic drag) and the compression due to the inside versus outside pressure difference. To calculate such stresses, the theory of Sanden and Guther was employed. As a result of the theory application, the authors found the number, size, and volume of the ribs. Such results are illustrated in Table I. The overall view of the double ellipsoid structure is visible in Fig.6.

Table I: Ribs radius, position and section.

Rib number	Rib radius [m]	Rib position [m]	Rib volume [m <sup>3</sup> ]
1	1,25	1,00	3,44E-03
2	1,70	2,00	4,72E-03
3	2,00	3,00	5,57E-03
4	2,21	4,00	6,17E-03
5	2,36	5,00	6,58E-03
6	2,45	6,00	6,84E-03
7	2,49	7,00	6,97E-03
8	2,49	8,00	6,97E-03
9	2,45	9,00	6,84E-03
10	2,36	10,00	6,58E-03
11	2,21	11,00	6,17E-03
12	2,00	12,00	5,57E-03
13	1,70	13,00	4,72E-03
14	1,25	14,00	3,44E-03

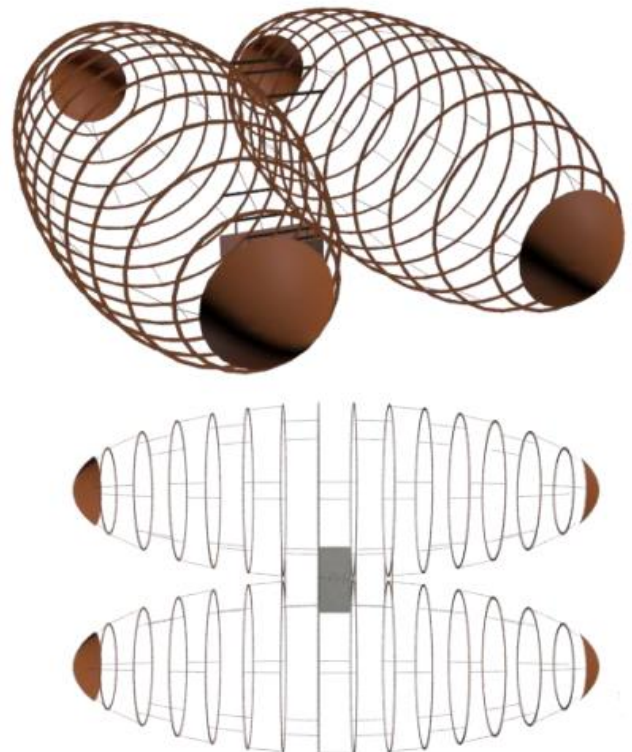


Fig. 6: View of the assembled double ellipsoid structure.

Glued on the shell, there is a polyurethane casing, whose main characteristics are lower thickness and density, lightness and resistance to mechanical stresses and to the action of ultraviolet rays. Its functions are to secure an aerodynamic shape to the mean and to protect the inner part. Moreover, for safety reasons, the possibility that a lightning can strike the airship was considered; Owing to the flammability characteristics of natural gas contained in the casing, a lightning would act as an ignition source for the fuel. Therefore it has been decided to realize an aluminum Faraday cage. Aluminum was chosen for its excellent electrical conductivity. In particular it has been suggested to use a 50x50 mm aluminum net realized with 3 mm diameter wires.

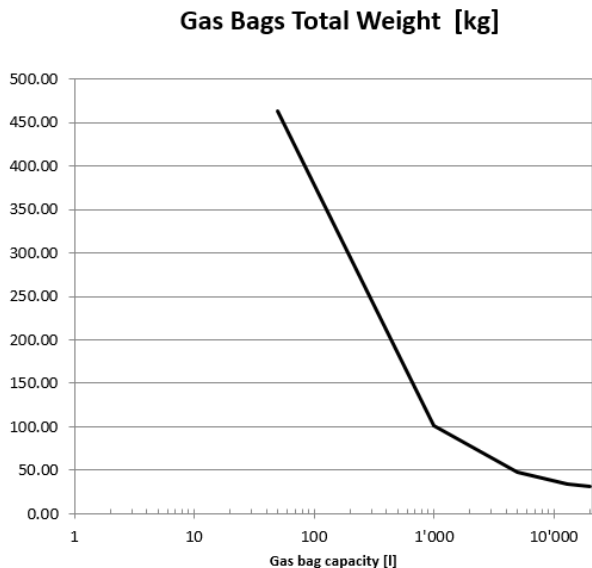


Fig. 7. Graph representing the relationship between the capacity of a single bag and the total weight.

For the gas bags material, the bi-axially oriented polyethylene terephthalate was identified, a plastic material of polyester family. The most important features of this material are the reduced density, the possibility to obtain very thin films (also 20µm) and the impermeability to gases. Commercially, gas bags in this material are available, with maximum capacity of 50 litres, therefore it is necessary to realize elliptical custom made bags in order to efficiently exploit the available volume and significantly reduce the weight (Fig. 7.).

The choice fell on 13 cubic meters capacity gas bags with 7.5 meters length and minor semi-axis equal to 1 meter. This solution involves a number of 12 gas bags for the helium storage; for safety reasons; the number of 12 gas bags is redundant, since the lift force is assured by the correct operation of only 10 out of 12 bags. Instead, the number of gas bags that contain natural gas is equal to 16.

IV. PROPULSION

The airship motion is assured by three propellers [4], of which one produces the thrust for propulsion and the two other act as thrusters and operate during maneuvers. The powertrain scheme [5, 6] is provided in Fig. 8. The internal combustion engine (of the “hot plug” typology) moves an alternator and, by means of a co-axial shaft, the main propeller. The two thrusters, moved by brushless electric motors, take power from the alternator.

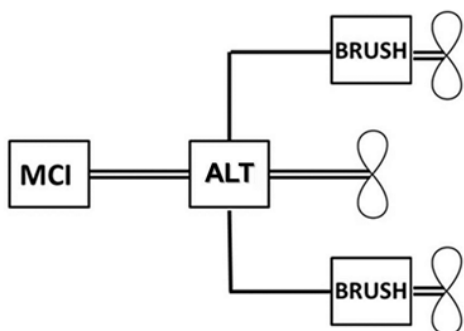


Fig. 8. Propulsion powertrain.

Although efficiently employable for medium-low powers ( $\leq 50$  kW), brushless motors have numerous advantages: reduced maintenance, great reliability, good performance, easy heat removal, high power/mass and power/size ratios, low acoustic noise and no need of special start devices.

Thanks to the rotary movement transmitted by the drive shaft, the propeller rotates to provide the forward thrust. The propeller is therefore the organ employed to accelerate the blimp up to the flight speed and to win the aerodynamic resistance which opposes to the motion.

The authors opted for the employ of two-bladed propellers, the most appropriate for engines providing low output powers. Propellers are made of carbon fiber, which combine mechanical resistance and low weight; moreover, the propellers are of the fixed geometry type, to obtain an advantageous ratio between performance and cost. For the sizing of the internal combustion engine it is necessary to calculate the force necessary to overcome the drag exerted on the vehicle in motion (Eq. 3).

$$F_R = \frac{1}{2} \rho_{air} C_x A v^2 k \tag{3}$$

Where:

- $F_R$  is the drag force expressed in N;
- $\rho_{air}$  is the air density at cruising altitude (900 m), expressed in  $kg/m^3$ ;
- $C_x$  is the airship drag coefficient;
- $A$  is the airship front area;
- $v$  is the airship design speed (40 km/h ), expressed in m/s;
- $k$  is a safety factor assumed to be 2.

$F_R$  is the force required by the propulsion propeller to move the airship at the set speed.

To size the propeller diameter, reference was made to the actuator disk theory developed by Rankine; the theory considers a steady stream, not viscous, incompressible and asymptotic  $V_\infty$  speed investing perpendicularly a circular area of infinitesimal thickness and diameter  $D$  (Fig. 9).

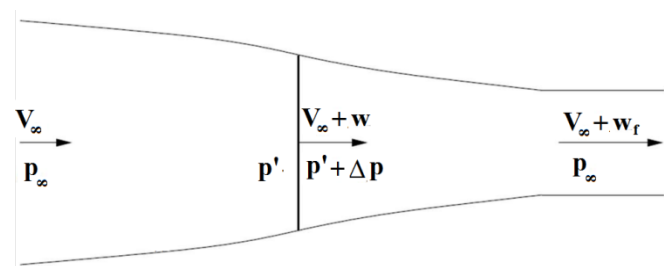


Fig. 9. Flow tube by the propeller.

It is assumed that the physical quantities in the flow tube are only a function of the axial coordinate  $z$ . It is possible to notice that speed increases along the  $z$  axis. In correspondence of the propeller axial position, the speed is increased by a quantity of  $w$ , corresponding to 40% of the upstream speed; downstream instead speed appears to be increased by 80%. It is also assumed that the disk does not produce a tangential speed component in the flow. With these assumptions, it is possible to obtain the propeller diameter necessary to sustain the airship at the speed set in the design phase (Eq. 4).



$$D = \sqrt{\frac{2 F_R}{\pi \rho (V_\infty + w) w}} \quad (4)$$

Where:

- $D$  is the propeller diameter, expressed in meters;
- $F_R$  is the force of the propeller, expressed in N;
- $\rho$  is the air density at cruising altitude (900 m), expressed in  $kg/m^3$ ;
- $V_\infty$  is the airship speed expressed in  $m/s$ ;
- $w$  is the speed increase by the propeller .

The application of the above exposed theory lead to a propeller diameter equal to 90 cm.

Then the power  $P$  associated to the propeller exerting on the airflow a force  $F_R$  has been found resolving the equation (Eq. 5)

$$P = [(V_\infty + w) F_R] / 1000 \quad (5)$$

Where:

- $P$  is the power required by the propeller, expressed in kW;
- 1000 is a conversion factor.

It is therefore possible to estimate the propeller efficiency by making the ratio between the power useful for motion (equal to the product between the propulsion force  $F_R$  and the vehicle speed  $V_\infty$ ) and the propeller power (Eq. 6).

$$\eta = (F_R V_\infty) / P = 1 / (1 + a) \quad (6)$$

Where:

- $\eta$  is the propeller efficiency;
- $a$  is the axial interference factor, equal to  $w/V_\infty$ .

This efficiency is around 0.75; therefore it is possible to determine the mechanical power required by the internal combustion engine (Eq. 7).

$$P_{mci1} = P/0.75 \quad (7)$$

To size the two thrusters, the vehicle rotational speed around the vertical axis is required as a design parameter. It was assumed to impose a 90 degrees rotation in 3 seconds. To size the thrusters, a fundamental quantity to be imposed is the distance between the thruster axes and the airship center of gravity. To calculate the force required for the rotational features above exposed, the following formula was employed (Eq.8).

$$F_m = 2 (J \dot{w}) / (w d) \quad (8)$$

Where:

- $F_m$  is the force required by the thrusters, expressed in N;
- $J$  is the moment of inertia of the airship set to be equal to a single ellipsoid, expressed in  $kg/m^2$ ;
- $\dot{w}$  is the angular acceleration expressed in  $rad/s^2$ . The acceleration value has been valued considering a triangle distribution and then assuming that the speed reaches the maximum value at time  $t' = t/2$ . The angular acceleration value is therefore estimated using the average velocity over time  $t'$  equal to  $\pi/12 rad/s$ ;

-  $d$  is the distance from the center of gravity, assumed equal to 5 meters;

- 2 is a safety factor.

At low rotational speeds the performance of the propellers decreases significantly; it can be considered a reference value of 0.3 for the efficiency. Using this data it is possible to determine the power that must be supplied by the electric motors for moving the propellers (Eq. 9) and the diameter of the latter (Eq. 10).

$$P_m = (F_m w d) / (1000 \eta_m) \quad (9)$$

Where:

- $P_m$  is the power that must be supplied by the electric engine, expressed in kW;
- $\eta_m$  is the propeller of maneuver performance;
- 1000 is a conversion factor.

$$D = \sqrt{\frac{2 P \eta_m^3 1000}{\pi \rho (w d)^3 (1 - \eta)}} \quad (10)$$

To go back to the power required to the internal combustion engine according to the power supply line used for the handling phases, the efficiencies of the electric motors and alternator need to be considered. For the brushless motors, the efficiency is very high and can be estimated as 0.9; also the generator efficiency can be assumed 0.90. Therefore the power that must be supplied by the internal combustion engine for maneuvers is calculated by the (Eq. 11).

$$P_{mci2} = P_m / (\eta_{mbr} \eta_{alt}) \quad (11)$$

Where:

- $\eta_{mbr}$  is the brushless motors efficiency;
- $\eta_{alt}$  is the alternator efficiency.

## V. STATIONS

It has been hypothesized to load the gas into the airship withdrawing it from a tank in which the gas is stored at a pressure of 30 bar. To determine the pressure that the gas must achieve in order to be placed in gas bags it must use the state equation of van der Waals. The objective is to determine a pressure such that the natural gas to the cruising altitude presents the same density as air, in order to provide zero upwards thrust. The application of van der Waals equation conducted on natural gas has led to consider a pressure of about 1.67 bar. To realize the pressure drop wanted, reference is made to a Natural gas Pressure reduction group of first stage as presented in Fig. 10. The regulation generally takes place by means of two lines of equal potential, one in operation and one as reserve and each consisting of two regulators, one in operation and one emergency, so that if one were to present an interruption for technical reasons, the other would begin to function. On each reduction line, there are a filter for purifying the gas from any impurities, a heat exchanger to cope with the lowering of temperature caused by the pressure drop which would cause problems to the system. These components are placed upstream of the

pressure reducing system, which is realized using a Joule Thomson valve (indicated as 4 in Fig. 10).

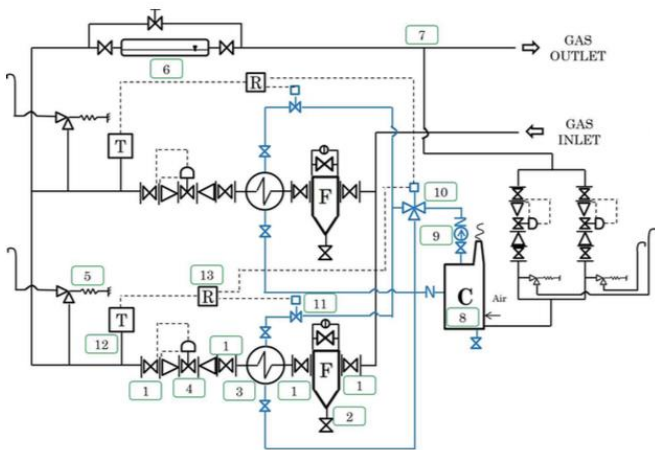


Fig. 10. Reduction of CNG pressure for transportation in airship.

In Fig. 10 is possible to notice several devices devoted to increase safety and a smooth operation:

- 1: shutoff valves
- 2: filters
- 3: heat exchangers to compensate CNG expansion cooling (isenthalpic expansion)
- 4: Joule Thomson expander
- 5: Safety Valves
- 6: Odorizers
- 7: Gas spill (for steam generators feeding)
- 8: Steam generators
- 9: Pumps
- 10: three-ways valves
- 11: Servo Valves (regulation)
- 12: Thermometers
- 13: Water flow measurers

The output pressure and temperature at which the gas will be introduced into the bags are imposed using a bayonet connection system similar to that used in the automation field to the cylinder trucks.

Regarding the discharge phase, it is assumed to download the gas into a tank and then enter into the low pressure network. Therefore it has considered 0.04 bar as reference pressure. In order to accomplish this, the use of a 2° stage industrial reduction is considered. Also in this case, the plant design solution provides two expansion lines: one for function and the other one for emergency. Upstream of the reduction system a filter is placed. It is also necessary to provide a line and an emergency regulator with safety and relief valve. The construction features of reduction and measurement cabins comply with the specifications of the D.M. 24/11/1984 "Fire Safety for the transport, distribution, storage and use of natural gas with a density no greater than 0.8".

## VI. MISSION PROFILE

In this section, the flight issues are presented. The route connecting the University Campus of Savona with the industrial area of Bene Vagienna, located in the province of Cuneo, has been considered as the mission. Ideally the mean will fly over the motorway A6 between the exits Savona and Fossano.

This is justified by the fact that theoretically the path is the one that has the lowest average altitude. To cover this distance, estimated in 80 km, a timeframe of about three hours has been considered, because airship cruising speed has been set around 40 km/h, but time of uploading and downloading of the airship has to be considered. To evaluate the cruising altitude, the elevation profile has been analyzed with the help of OpenGTS software. Then the obtained values have been increased by 150 meters to obtain the maximum altitude at which the airship should travel in safety conditions.

In the experiment, made using a GPS to collect the possible path, is possible to notice that the maximum height is near 900 meters above sea level. Obviously, to avoid having to adjust the buoyancy in flight, the cruising altitude has been set to 900 meters.

For the mission regulations the authors have relied on the ENAC norms for remote controlled vehicles [7]. The airship is identified with the acronym SAPR because it is an Aircraft Remote Piloting System utilized in specialized, scientific, experimental and research operations. In particular it is a SAPR with an operative takeoff mass between 25 kg and 150 kg. This implies that operations are considered to be of critical nature. It is also adopted a remote controlled BVLOS (Beyond Visual Line Of Sight), as the operations are conducted at a distance that does not allow the remote pilot to remain in direct and constant eye contact with the airship. In the delineation of the mission the organization of neighboring airspaces and airports has been considered. Indeed, each airport has limited or prohibited traffic areas to ensure safety; a distinction can be made between CTR (Control Area) and ATZ (Aerodrome Traffic Zone). The first acronym indicates a controlled air space that extends from the soil surface up to a specific upper limit. Its lateral limits contain the portions of routes of take-off and landing near the airport. In these areas drones flight is allowed up to a maximum height of 70 meters. The second acronym identifies an airspace of defined size established around an airport for the protection of take-off and landing operations; there drones flying is forbidden (Fig. 11).



Fig. 11. Map on trafficking carried out by the drone. Brown represents the ATZ and blue the CTR.

## VII. EMERGENCY MANAGEMENT

In the mission evaluation some measures of fundamental importance have been taken in order to deal safely with the most relevant emergency scenarios. Three of them have been considered: piercing of the bags containing the lift gas, reliability of the powertrain and risks related to natural gas flammability.

Regarding the possibility that problems to gas bags containing helium might occur during flight, two solutions have been considered in order to mitigate the risk. As already said, the authors have decided to oversize the number of helium bags; this allows to have some spare useful bags to compensate any dispersion of part of the flotation gas. Moreover, each bag is equipped with pressure switches able to provide the control centre, in real time, information about the state of the gas bags. In this way, if problems should occur to the gas bags, it would be possible to promptly intervene to safely land the mean and provide for the maintenance operations. Usually, in aeronautical sector, means and control systems are equipped with redundant components for each of the most important operations that must always be guaranteed for the conduction of operations in complete safety. In this aspect, the powertrain adopted in this project presents a weak point; Indeed, the propulsion propeller and the thrusters are guaranteed by the operation of the internal combustion engine. This choice is dictated by design, economic and environmental reasons, and for a prototype, this problem is not particularly relevant. The possible use of a second internal combustion engine in fact would require higher size and a different amount of lift gas owing to the overall weight increase. To reduce the malfunction of the internal combustion engine, it is possible to adopt one characterized by high quality standards, such as:

- Ability to work in continuous service;
- High-quality mechanical materials;
- Overheating resistance;
- High performance.

The natural gas presence rises the problem of a potentially explosive mixture with oxygen; therefore safety measures must be adopted to prevent from the formation of an ignition source. For the analysis of this issue it was considered a maximum air temperature in the internal blimp volume of around 50° C. A potential ignition may be caused by a possible friction between the cage and the valves that could give rise to sparks. To eliminate these risks it is opted for the application of the cage above the polyurethane casing. In this way, the ignition energy can be generated only from problems related to electrical equipment. To reduce also these risks it was decided to realize electrical systems with technology suitable for explosive atmospheres and to employ elastomeric materials able to function under the effect of fire.

After dealing with prevention systems to be adopted in the airship, some safety systems have been studied, in the event that a fire should be triggered. Obviously the propagation of a fire inside the airship would have destructive effects, so it is necessary to use materials able to prevent the spread of fire. All the materials used must therefore be manufactured to meet the flammability requirements of UL 94 5V test.

## VIII. CONCLUSIONS

This research study has shown that the transport of natural gas via airship is potentially achievable. The airships are currently able to give (and probably will be even more in the future) effective responses to many needs in many areas. Currently, several countries are active in the industry with companies that produce or operate airships. Some specific features of the airship make it particularly interesting:

- Great autonomy and durability in flight: the lift force is not generated by aerodynamics but by buoyancy, thus saving fuel;

- High load: increasing the amount of lift gas can greatly increase the transport capacity. In addition, the large internal space provides low size loads or forms incompatible with most of the other means of transport;

- Energy efficiency: in the airship, being the lift assured by gas, engines are used only to move, this results in energy consumption per hour of flying extremely low. Also it can cover the surface of the airship with a large solar panel which allows to minimize the use of non-renewable resources.

- Low environmental impact (emissions, noise, turbulence): low power consumption has the immediate reflection of a lower environmental impact. In fact, the levels of air and noise pollution are almost negligible with respect to a traditional aircraft.

- Ability to carry out operations in areas without airports: airship can land and take off vertically, therefore it doesn't need long runways. This does not mean that it can operate without an underlying infrastructure, which are instead necessary.

- Safety: security is guaranteed by the possibility to remain in flight even in case of all engines shutdown, the possibility to land (and to make emergency supplies) even in the absence of airports, the low speed to the moment of landing and the take-off, the poor sensitivity to certain atmospheric phenomena such as fog.

Also innovations in aviation have allowed an improvement of the airship features:

- Progress in meteorology, both understanding of atmospheric phenomena such as real-time availability of data on the entire planet's climate, allow higher levels of safety;

- Technological advances: the introduction of GPS overcomes one of the major difficulties of navigating of historical airships, which is determining the vehicle position in the absence of reference points;

- Improvement of structural materials: new aluminum alloys, titanium, carbon fiber, Kevlar, composite materials;

- Improvement of materials for the casing: replacement of tissues and natural membranes with synthetic materials such as nylon, polyester, polyurethane.

These allow considerable savings in the weight of a component that constitutes considerable part of the mass of an airship, longer life, lower permeability to gases and lower maintenance requirements.

- Reliability, efficiency and high power to mass ratio of the "hot plug" internal combustion engine.

- Process automation;

- Remote Steering: possibility of cost and weight reduction for numerous tasks and missions to face with risk levels otherwise unacceptable.

Based on these considerations, it is believed that a greater knowledge of the airships would be required, since it is an unexplored territory or under-exploited with considerable potential for improvement and growth. Moreover a study of

the issues shows how unfounded are the historical legacies that lead to associate the airship to poor security. For a return of the airship to its former glory we should make targeted investments aimed initially at improving knowledge on the matter and to form specialized and then produce adequate technical infrastructure required to refine the construction and operational techniques.

Future developments will face the task to build a down-scaled model [8] to obtain experimental data to be compared with the theoretical ones found in this study; moreover, deeper logistics [9] and simulation [10] studies will be carried on including the possibility of an on-line real-time simulation for supporting navigation in open-sea [11].

## REFERENCES

- [1] G. Bruzzone, R. Mosca, A. Orsoni, R. Revetria, Simulation-based VV&A Methodology for HLA Federations: an Example from the Aerospace Industry. Proceedings – Simulation Symposium 2002.
- [2] L. Damiani, R. Revetria, P. Giribone, G. Guizzi, Simulative Comparison between Ship and Airship for the Transport of Waste Natural Gas from Oil Wells, 2015 SoMeT - XVII Summer School "Francesco Turco", Naples.
- [3] P. Giribone, R. Revetria, A. Testa, G. Vernengo, E. Rizzuto, R. Longo, A Simulation Based Methodology for Supporting CNG Ship Design, Recent Advances in Mathematics, ISBN: 978-1-61804-158-6.
- [4] M. Acanfora, L. Lecce, On the Development of the Linear Longitudinal Model for Airships Stability in Heaviness Condition, 2011, The Journal of Aerospace Science, Technology and Systems.
- [5] J. Dellachà, L. Damiani, M. Repetto, A. Pini Prato, Dynamic Model for the Energetic Optimization of Turbocompound Hybrid Powertrains, Energy Procedia 45 (2014) 1047 – 1056.
- [6] G. Ilieva, J. Páscoa, A. Dumas, M. Trancossi, A Critical Review of Propulsion Concepts for Modern Airships, 2012, Open Engineering. Volume 2, Issue 2, Pages 189–200, ISSN (Online) 2391-5439.
- [7] <https://www.enac.gov.it>. Contains rules for flight control and supervision in Italy and EU countries. Last visited July 2017.
- [8] G. Capitta, L. Damiani, S. Laudani, R. Revetria, E. Morra, Mechanical Design of an Innovative Method for CNG Transporting over Long Distances: Logistics, Executive and Operative Aspects”. Lecture Notes in Engineering and Computer Science: Proceedings of The International MultiConference of Engineers and Computer Scientists 2017, IMECS 2017, 15-17 March, 2017, Hong Kong, pp 780 785.
- [9] E. Briano, C. Caballini, P. Giribone, R. Revetria, Using System Dynamics for Short Life Cycle Supply Chains Evaluation. 2010, Proceedings of Winter Simulation Conference.
- [10] L. Cassettari, R. Mosca, R. Revetria, Monte Carlo Simulation Models Evolving in Replicated Runs: A Methodology to Choose the Optimal Experimental Sample Size. 2012, Mathematical Problems in Engineering.
- [11] L. Damiani, P. Giribone, R. Revetria, A. Testa, “An Innovative Model for Supporting Energy-based Cost Reduction in Steel Manufacturing Industry using Online Real Time Simulation” Lecture Notes in Engineering and Computer Science: Proceedings of The World Congress on Engineering and Computer Science 2014, WCECS 2014, 22-24 October, 2014, San Francisco, USA, pp 1075-1081.
- [12] R. Baldacci “Scienza delle Costruzioni, Volume II”, Unione Tipografico-Editrice Torinese UTET. 1997. Turin, Italy. ISBN 88-02-04634-4.
- [13] A. R. Bryant., 1954. Hydrostatic pressure buckling of a ring-stiffened tube. Report R-306, Naval Construction Research Establishment, UK.
- [14] P. K. Das, D. Faulkner, R. A. Zimmer Selection of robust strength models for efficient design of ring and stringer stiffened cylinders under combined loads Proceedings of the 11th International Conference on Offshore Mechanics and Arctic Engineering, Calgary, Canada (1992), pp. 417-428, 7-12 June 1992
- [15] L. B. Wilson The elastic deformation of a circular cylindrical shell supported by equally spaced ring frames under uniform external pressure Transactions of the Royal Institution of Naval Architects, 108 (1966), pp. 63-72